JOC Article

Predicting the UV−Vis Spectra of Tetraarylcyclopentadienones: Using DFT Molecular Orbital Energies to Model Electronic Transitions of Organic Materials

Robert G. Potter and Thomas S. Hughes*

Department of Chemistry, Cook Physical Sciences Building, 82 University Place, University of Vermont, Burlington, Vermont 05405

thomas.s.hughes@uvm.edu

Received August 15, 2007

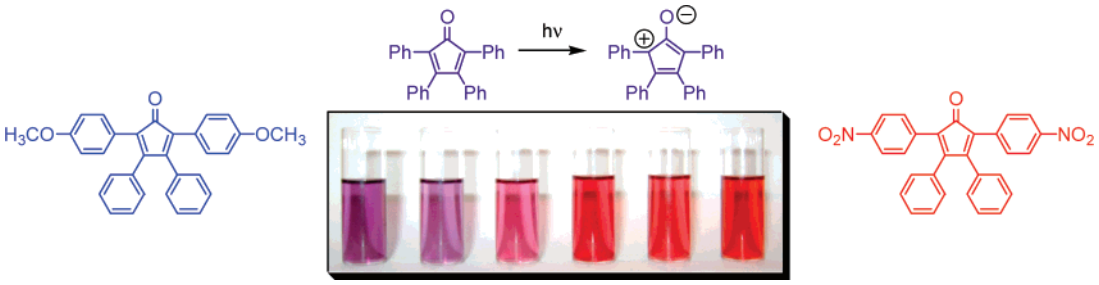

Tetraphenylcyclopentadienone, due to its intrinsically low HOMO−LUMO gap, has been suggested as a valuable repeat unit in conducting polymers for nanoscale electronics. The HOMO and LUMO of tetraphenylcyclopentadienone appear to be associated with the relevant π orbitals of unsubstituted cyclopentadienone. Using previously developed carbonylative coupling reactions, a series of tetraarylcyclopentadienones was synthesized, accessing a range of substituents not previously available. The UV−vis spectra of these molecules were compared to their calculated wave functions and predicted transitions. A quantitative structure−activity relationship was discovered that may greatly simplify prediction of band gaps for oligomers and polymers built from these tetraarylcyclopentadienones.

Introduction

Molecules that contain strongly absorbing chromophores not only have found use as pigments and dyes, but are also of current interest as building blocks for low band gap conjugated oligomers and polymers.[1] Such materials are of particular interest for their use as "organic metals",[2] as semiconductors for use in field effect transistors,[3] and as emissive or absorbing materials for LEDs[4] or photovoltaics.[5] In particular, the fulvalene and cyclopentadienone scaffolds have been suggested as useful repeat units[6] due to the low HOMO−LUMO gap of these monomers and subsequent reduction of the band gap upon the increase of conjugation upon oligomerization.[7,8] Cyclopentadienones in particular are also synthetic precursors of phenylenes,[9]

(1) Bendikov, M.; Wudl, F.; Perepichka, D. F. *Chem. Rev.* **2004**, *104*, 4891. Skabara, P. J.; Berridge, R.; McInnes, E. J. L.; West, S. J. C.; Hursthouse, M. B.; Müllen, K. *J. Mater. Chem.* **2004**, *14*, 1964. Geerts, Y.; Klärner, G.; Müllen, K. In *Electronic Materials*: *The Oligomer Approach*; Müllen, K., Wegner, G., Eds.; Wiley-VCH: Weinheim, Germany, 1998. Enkelman, V. In *Electronic Materials*: *The Oligomer Approach*; Müllen, K., Wegner, G., Eds.; Wiley-VCH: Weinheim, Germany, 1998.

(2) Reddinger, J. L.; Reynolds, J. R. *Adv. Polym. Sci.* **1999**, *145*, 57. Coropceanu, V.; Cornil, J.; da Silva Filho, D. A.; Olivier, Y.; Silbey, R.; Brédas, J.-L. *Chem. Rev.* **2007**, *107*, 926. Shirota, Y.; Kageyama, H. *Chem. Rev.* **2007**, *107*, 953.

(3) Garnier, F. In *Electronic Materials*: *The Oligomer Approach*; Müllen, K., Wegner, G., Eds.; Wiley-VCH: Weinheim, Germany, 1998. Murphy, A. R.; Fréchet, J. M. J. *Chem. Rev.* **2007**, *107*, 1066.

(4) Harrison, M. G.; Friend, R. H. In *Electronic Materials*: *The Oligomer Approach*; Müllen, K., Wegner, G., Eds.; Wiley-VCH: Weinheim, Germany, 1998. Robertson, N. *Angew. Chem.* **2006**, *45*, 2338. Shih-Chun Lo, S.-C.; Burn, P. L. *Chem. Rev.* **2007**, *107*, 1097.

(5) Tang, C. W. *Appl. Phys. Lett.* **1986**, *48*, 183. Saricifiti, N. S.; Smilowitz, L.; Heeger, A. J.; Wudl, F. *Science* **1992**, *258*, 1474. Günes, S.; Neugebauer, H.; Sariciftci, N. S. *Chem. Rev.* **2007**, *107*, 1324.

(6) Wudl, F. *Humphrey Symposium*; University of Vermont: Burlington, VT, Sept 2006.

(7) Gierschner, J.; Cornil, J.; Egelhaaf, H.-J. *Adv. Mat.* **2007**, *19*, 173.

(8) Salzner, U. *Curr. Org. Chem.* **2004**, *8*, 569. Cornil, J.; Beljonne, D.; Brédas, J. L. In *Electronic Materials*: *The Oligomer Approach*; Müllen, K., Wegner, G., Eds.; Wiley-VCH: Weinheim, Germany, 1998.

(9) Wu, J.; Pisula, W.; Müllen, K. *Chem. Rev.* **2007**, *107*, 718. Morgenroth, F.; Reuther, E.; Müllen, K. *Angew. Chem., Int. Ed.* **1997**, *36*, 631. Iyer, V. S.; Weheimer, M.; Brand, J. D.; Keegstra, M. A.; Müllen, K. *Angew. Chem., Int. Ed.* **1997**, *36*, 1604.

10.1021/jo701676x CCC: $40.75
Published on Web 03/26/2008

which are target materials for the same applications. It is therefore highly desirable to obtain a detailed understanding of the electronic structure of the tetraarylcyclopentadienone moiety, in particular the HOMO−LUMO gap, and how that gap can be tuned by substitution of the aryl groups. Herein is presented a spectroscopic and molecular orbital study of a series of substituted tetraarylcyclopentadienones (TACPDs).

Recent developments in time-dependent density functional theory[10] have allowed predictions of electronic transitions of conjugated oligomers,[11] although systematic errors arising from long-range electron correlation are problematic for longer oligomers.[7] However, if CI calculations indicate that certain transitions are primarily single-electron excitations, simple DFT can in principle give reasonable predictions of the transition energies. This has been demonstrated by several groups for a diverse set of molecules.[12] Ab initio MO and DFT computations were therefore performed to model these transitions, and to determine the level of theory required to predict the magnitude of the HOMO−LUMO gap. A clear relationship between the calculated electronic structure and the spectra was identified. These results not only add to the wealth of experimental data reported by other groups,[13] but also provide a more quantitative explanation of the substituent effects on the electronic transitions of TACPDs that may guide the design of TACPD oligomers.

There are few reported examples of TACPDs bearing electron-withdrawing groups, and any investigation of the effect of substituents on the electronic spectra of TACPDs should include members of this class. The use of appropriate carbonylative coupling reactions has allowed access to previously unreported TACPDs with a range of electron-donating or electron-withdrawing groups. This extended library of TACPDs has allowed investigation of the electronic properties, and in particular the electronic transitions.

Tetraphenylcyclopentadienone (**1a**), first synthesized by Dilthey and co-workers,[14] is a stable analogue of the very unstable cyclopentadienone **2** that was not isolated until years later by matrix isolation in argon.[15] The reactivity of the parent compound can be explained by the presence of an antiaromatic valence bond (VB) structure (Scheme 1) as one of the primary resonance forms, a model that has been supported by DFT calculations.[16] The compound spontaneously undergoes an intermolecular Diels−Alder cycloaddition with another molecule

SCHEME 1. Tetraarylcyclopentadienones Synthesized and Parent Cyclopentadienone

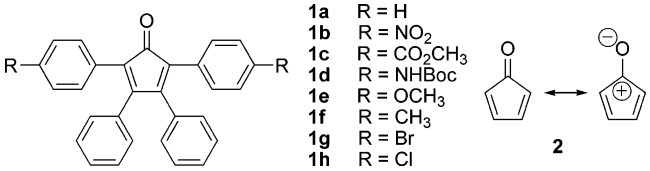

of **2** in the absence of a solid matrix.[17] Substitution of the cyclopentadienone ring with phenyl rings provides enough steric bulk to prevent intermolecular interaction to the extent that **1a** is stable at modestly high temperatures, but will react at high temperature when an appropriate dienophile is present.[18]

The UV−vis spectra of substituted TACPDs have been recorded earlier, and the electronic transitions have been assigned to different valence-bond structures associated with the exited states.[13] While VB theory is well-known for its utility for describing reaction mechanisms and other circumstances where strict knowledge of electronic structure is not necessary, the quantitative nature of molecular orbital (MO) theory and its derivation from first principles make it a better suited model for the analysis and prediction of electronic structure and UV−vis transitions. A marriage of VB and MO theories has long been pursued due to the valuable and quantifiable predictions of the two models.[19]

The purpose of this study is to readdress the electronic spectra of TACPDs by using an MO description of the ground and excited states which may quantitatively predict the observed phenomena. The relationship between the electronic properties of the substituent, which could in principle be modeled as a function of group electronegativity[20] or a Hammett linear free energy parameter,[21] and the corresponding absorption maxima were analyzed to find a quantitative relationship. To describe the effect of various substituents on the π MOs of the TACPDs, the correlations between the molecular orbitals of **1a** and the well-known parent compound **2** were established.

Results and Discussion

Synthesis of Substituted Tetraarylcyclopentadienones. By using carbonylative coupling reactions developed by Collman,[22] des Abbes,[23] and van Leusen[24] followed by Knovenagel

(10) Casida, M. E.; Casida, K. C.; Salahub, D. R. *Int. J. Quantum Chem.* **1998**, *70*, 933. Burke, K.; Werschnik, J.; Gross, E. K. U. *J. Chem. Phys.* **2005**, *123*, 062206.

(11) Salzner, U.; Karalti, O.; Durdağı, S. *J. Mol. Model.* **2006**, *12*, 687. Zade, S. S.; Bendikov, M. *Org. Lett.* **2006**, *8*, 5243. Fratiloiu, S.; Grozema, F. C.; Koizumi, Y.; Seki, S.; Saeki, A.; Tagawa, S.; Dudek, S. P.; Siebbeles, L. D. A. *J. Phys. Chem. B* **2006**, *110*, 5984. Toivonen, T. L. J.; Hukka, T. I. *J. Phys. Chem. A* **2007**, *111*, 4821.

(12) van Slageren, J.; Stufkens, D. J.; Zalis, S.; Klein, A. *J. Chem. Soc. Dalton Trans.* **2002**, 218. Brière, J.-F.; Côté, M. *J. Phys. Chem. B* **2004**, *108*, 3123. Namai, H.; Ikeda, H.; Kato, N.; Mizuno, K. *J. Phys. Chem. A* **2007**, *111*, 4436.

(13) (a) Thaller, F. J.; Trucker, D. E.; Becker, E. I. *J. Am. Chem. Soc.* **1951**, *73*, 228. (b) Coan, S. B.; Trucker, D. E.; Becker, E. I. *J. Am. Chem. Soc.* **1953**, *75*, 900. (c) Shapiro, E. L.; Becker, E. I. *J. Am. Chem. Soc.* **1953**, *75*, 4769. (d) Coan, S. B.; Trucker, D. E.; Becker, E. I. *J. Am. Chem. Soc.* **1955**, *77*, 60.

(14) (a) Dilthey, W.; Braun, W.; Trösken, O. *J. Prakt. Chem.* **1933**, *139*, 1.

(15) (a) Chapman, O. L.; McIntosh, C. L. *J. Chem. Soc. D* **1971**, 770. (b) Maier, G.; Franz, L. H.; Hartan, H.-G.; Lanz, K.; Reisenauer, H. P. *Chem. Ber.* **1985**, *118*, 3196.

(16) Najafian, K.; Schleyer, P. L.; Tidwell, T. T. *Org. Biomol. Chem.* **2003**, *1*, 3410.

(17) (a) Depuy, C. H.; Lyons, C. E. *J. Am. Chem. Soc.* **1960**, *82*, 631. (b) Hafner, K.; Goliasch, K. *Angew. Chem.* **1960**, *72*, 781.

(18) (a) Dilthey, W.; Thewalt, I. *Chem. Ber.* **1934**, *67*, 1959. (b) Grummitt, O.; Klopper, R. S.; Blenkhorn, C. W. *J. Am. Chem. Soc.* **1942**, *64*, 604. (c) Dilthey, W.; Hurtig, G.; Passing, H. *J. Prakt. Chem.* **1940**, *156*, 27.

(19) Randic, M. *Chem. Rev.* **2003**, *103*, 3449.

(20) (a) Pearson, R. G. *Proc. Natl. Acad. Sci.* **1986**, *83*, 8440. (b) De Proft, F.; Langenaeker, W.; Geerlings, P. *J. Phys. Chem.* **1993**, *97*, 1826. (c) Leyssens, T.; Geerlings, P.; Peeters, D. *J. Phys. Chem. A* **2006**, *110*, 8872.

(21) (a) Hammett, L. P. *Chem. Rev.* **1935**, *17*, 125. (b) Hammett, L. P. *J. Am. Chem. Soc.* **1937**, *59*, 96. (c) Hammett, L. P. *Trans. Faraday Soc.* **1938**, *34*, 156. (d) Hammett, L. P. *Physical Organic Chemistry*; McGraw-Hill Book Co.: New York, 1940.

(22) (a) Collman, J. P.; Winter, S. R.; Clark, D. R. *J. Am. Chem. Soc.* **1972**, *94*, 1788. (b) Collman, J. P. *Acc. Chem. Res.* **1975**, *8*, 342. (c) Collman, J. P.; Finke, R. G.; Cawse, J. N.; Brauman, J. I. *J. Am. Chem. Soc.* **1977**, *99*, 2515.

(23) (a) Tanguy, G.; Weinberger, B.; des Abbayes, H. *Tetrahedron Lett.* **1984**, *25*, 5529. (b) des Abbayes, H.; Clément, J.-C.; Laurent, P.; Tanguy, G.; Thilmont, N. *Organometallics* **1988**, *7*, 2293.

(24) Possel, O.; van Leusen, A. M. *Tetrahedron Lett.* **1977**, *48*, 4229. van Leusen, D.; van Leusen, A. M. *Org. React.* **2001**, *57*, 417.

SCHEME 2. Synthesis of Series 1b−h

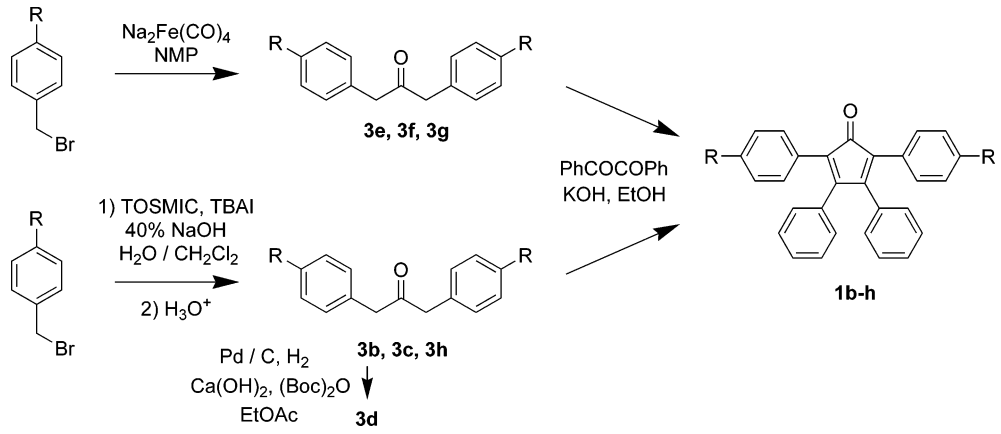

condensations,[25] a variety of different TACPDs were synthesized to expand the library of UV−vis data previously reported for these compounds (Scheme 2). A convenient method of synthesizing TACPDs involves the ethanolic potassium hydroxide-mediated Knovenagel condensation between a benzil and a 1,3-diaryl-2-propanone.[13,14] The placement of substituents on the aryl rings in **1** simply requires the use of appropriately substituted benzils or 1,3-diaryl-2-propanones. Since Becker observed a greater shifting of the longest wavelength transition upon substitution of the 2- and 5-phenyl rings,[13c] substitution of the 1,3-diaryl-2-propanone synthons was undertaken.

Preparation and use of the Collman reagent toward the preparation of 1,3-diaryl-2-propanones **3** from the corresponding benzyl bromides has been reported earlier.[26] The yields of **3** were moderate to high when neutral or electron-donating substituents were present, but low to zero when electron-withdrawing substituents were present. Strict purification of all starting materials and solvents was necessary for the synthesis and reactions of $Na_2Fe(CO)_4$ toward the synthesis of **3e**, **3f**, and **3g**. To avoid the poor yields of the Collman couplings that give **3b** and **3c**, which bear nitro and methyl ester groups, respectively, the tosylmethyl isocyanide-mediated carbonylative coupling methodology of van Leusen was used with benzyl bromides bearing these strongly electron-withdrawing groups. Ketones **3b**, **3c**, and **3h** were synthesized by treating 2 equivalents of 4-nitrobenzyl bromide, 4-methoxycarbonylbenzyl bromide, and 4-chlorobenzyl bromide, respectively, with base and tosylmethylisocyanide under phase-transfer conditions, followed by acid hydrolysis of the resulting dibenzyltosylisocyanides. To probe the effect of strongly electron-donating substituents on the optical spectra of TACPDs, an amino-substituted 1,3-diaryl-2-propanone was desired. However, the difficulty encountered in preparing 4-aminobenzyl bromide necessitated an alternate route involving the reductive hydrogenation of **3b**, which unfortunately gave a complex mixture of oligomeric products that appeared to involve the condensation of the reduced amino groups with the carbonyl groups. Addition of di-*tert*-butyl dicarbonate to the hydrogenation mixture did afford the Boc-protected diamine **3d** in quantitative yield from **3b**.

The syntheses of **1b−h** were conducted with KOH in refluxing ethanol. Quenching the reaction with a mild acid followed by simple aqueous extraction and column chromatography afforded TACPDs **1b−h**. It should be noted that THF was substituted as solvent in the synthesis of **1c** to avoid transesterification of the ester moiety with the solvent. Yields of the Knovenagel condensations were moderate to high in most cases, and the products are stable for over a year if stored in the solid phase. However, solutions of many of these compounds decompose within weeks.

UV−Vis Spectroscopy of Tetraarylcyclopentadienones. UV−vis spectra for the substituted TACPDs are shown in Figure 1. All of the spectra were recorded in dioxane, at concentrations of 0.02−0.04 mmol/L. Each spectrum was fitted by using a sum of Gaussian functions;[27] the root-mean-square error of the sum of Gaussians compared to the raw spectrum was minimized as the height, width, and λ_{max} of each Gaussian was varied. The number of Gaussians used to fit each spectrum was determined by evaluating the root mean square; if no appreciable improvement in the fit was observed upon adding an additional Gaussian function, the next lowest number of functions was used.

The resulting absorption maxima are given in Table 1, along with the fitted extinction coefficients. All of the TACPDs exhibited three electronic transitions, which we have designated as λ^1 through λ^3. A fourth absorption maximum, λ^4, was observed for all of the TACPDs except for **1a** and **1f**. Each of these absorption maxima changed upon substitution of the para positions of the 2- and 5-phenyl rings. The features at 210 nm in all of the spectra recorded were fitted in each spectrum by a Gaussian function with a λ_{max} of 182 nm and a very large extinction coefficient, which suggests they correspond to the dioxane solvent.

The lowest energy transitions, λ^1, exhibited a bathochromic shift of 52 nm upon substitution of the electron-deficient TACPD, **1b**, with a λ^1_{max} of 492.5 nm, to the electron-rich **1d**, with a λ^1_{max} of 544.7 nm. The extinction coefficients varied from 1300 to 2000 L mol^{-1} cm^{-1}, and showed no correlation to the electron demand of the substituents. The second-lowest energy transitions, λ^2, exhibited a 53 nm bathochromic shift, of larger energy, with increasing electron-donating capacity of the substituent, from 323.5 nm for electron-poor **1b** to 376.1 nm for electron-rich **1d**. The spectrum of **1e** had previously been measured separately in isooctane and benzene,[13d] which allowed the observation of absorptions at 370 and 340 nm, respectively. In dioxane, two closely overlapping absorptions at 375 and 329 nm were fit with the Gaussian functions. A similar pair of absorptions was observed in dioxane for **1d**,

(25) Johnson, J. R.; Grummitt, O. *Organic Syntheses*; Wiley: New York, 1955; Collect. Vol. III, p 806.
(26) Potter, R. G.; Hughes, T. S. *Org. Lett.* **2007**, *9*, 1187.
(27) Hu, Y.; Liu, J.; Li, W. *Anal. Chim. Acta* **2005**, *538*, 383.

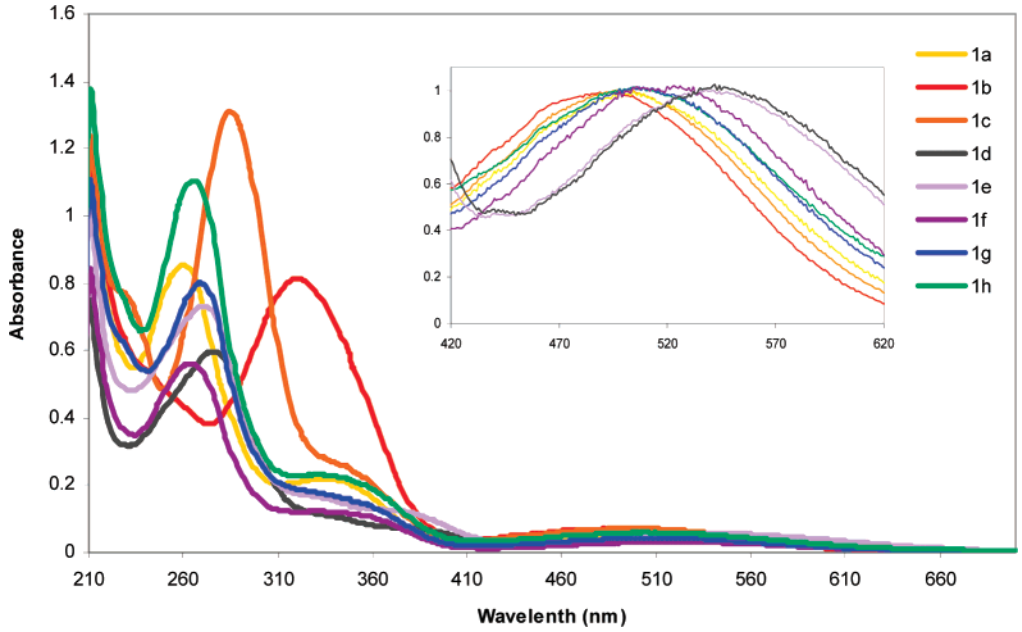

FIGURE 1. UV−vis spectra of **1a** through **1h** in dioxane. The inset shows the visible region of the spectra, and λ^1_{max} for each compound.

TABLE 1. Absorption Maxima and Extinction Coefficients for UV/VIS Spectra of 1a−h

compd	λ^1_{max}[a]	ϵ^1	λ^2_{max}	ϵ^2	λ^3_{max}	ϵ^3	λ^4_{max}	ϵ^4
1a (R = H)	503.8	1410	331.6	7080	259.4	26000		
1b (R = NO_2)	492.5	1960	323.5	7260	321.1	14700	248.9	9530
1c (R = CO_2CH_3)	496.0	1950	341.0	6720	284.3	35000	233.5	14900
1d[b] (R = NHBoc)	544.7	1960	376.1	3060	277.9	25300	242.9	12100
1e[b] (R = OCH_3)	539.7	1650	375.3	3160	276.5	7390	255.9	16800
1f (R = CH_3)	518.1	1340	338.6	5330	262.2	23300		
1g (R = Br)	513.0	1330	345.2	4620	271.1	10000	253.7	17100
1h (R = Cl)	510.0	1910	330.7	7700	264.5	33800	231.7	3560

[a] λ_{max} reported in nm, and ϵ in L mol^{-1} cm^{-1}. [b] **1d** and **1e** also exhibited absorptions at 328.5 and 319.7 nm with extinction coefficients of 3950 and 4250 L mol^{-1} cm^{-1}, respectively.

which also bears electron-donating substituents. The large range of λ^2_{max} observed in this set of TACPDs makes it clear that this transition is affected by substituents on the 2- and 5-phenyl rings, contrary to what was claimed earlier[13b,d] on the basis of a more limited set of spectra. Although all substituents shift the λ^3_{max} 257 nm absorption of the unsubstituted TACPD **1a** bathochromically, again contrary to previous claims,[13d] a clear relationship between λ^3_{max} and both the position and electron-donating capacity of the substituent was not evident in this larger set of substituted TACPDs. It should be noted that λ^3 for **1b** initially appeared to be absent, but the broad absorption maximum at ~323 nm for **1b** was fitted well by the sum of two gaussians, one centered at 321 nm and the other at 323 nm. To develop a tool for quantitatively predicting the spectra of TACPDs, in particular the long wavelength transition λ^1, the molecular orbitals and electronic transitions of **1a** and its parent compound **2** were calculated.

Electronic Structure and Electronic Transitions of Tetraarylcyclopentadienones. TACPDs can be considered as perturbations of the cyclopentadienone core **2** by substitution of each hydrogen with an aryl ring, which can potentially lower the C_{2v} symmetry of **2** depending on their orientation. To demonstrate this descent in symmetry, consider **2** substituted with four phenyl rings that are each perpendicular to the inner cyclopentadienone ring, such that the dihedral angle $\theta = 90°$. This molecule consists of two orthogonal π frameworks, one isolobal[28] to the unsubstituted **2**, and one that can be treated as the "ligand group" surrounding **2**. Both **2** and this structure with orthogonal π systems (**1a(*C*$_{2v}$)**) are defined by the C_{2v} point group. The four frontier π MOs of cyclopentadienone are depicted in Figure 2, as are the four frontier π MOs of **1a(*C*$_{2v}$)**, which contain components of these MOs from the cyclopentadienone core mixed with very small contributions of the orthogonal π MOs from the pendent phenyl groups. A significant gap exists between the highest occupied and the lowest unoccupied π MOs of **2** and **1a(*C*$_{2v}$)** that places the electronic transition in the UV manifold. The HF/6-31G(d)//B3LYP/6-31G(d) energies and geometries are shown for each of the MOs involved, and agree with previous experimental data for **2**.[29]

As the phenyl rings are rotated with respect to the plane of the cyclopentadienone core, the π orbitals of the two types of rings begin to mix. The orbitals and energies of **1a** shown to the right of Figure 2 are for the minimum energy structure, in which the less sterically crowded 2- and 5-phenyl rings have a 37° dihedral angle with respect to the cyclopentadienone core, and the more sterically crowded 3- and 4-phenyl rings have a dihedral angle of 52°. The gray lines indicate MOs of **1a(*C*$_2$)** that arise from small contributions of the cyclopentadienone π orbitals mixing with the pendent phenyl π orbitals, while the black lines indicate the frontier orbitals of **1a(*C*$_2$)** that are

(28) Hoffmann, R. Nobel Lecture, 1981.
(29) Koenig, T.; Smith, M.; Snell, W. *J. Am. Chem. Soc.* **1977**, *99*, 6663.

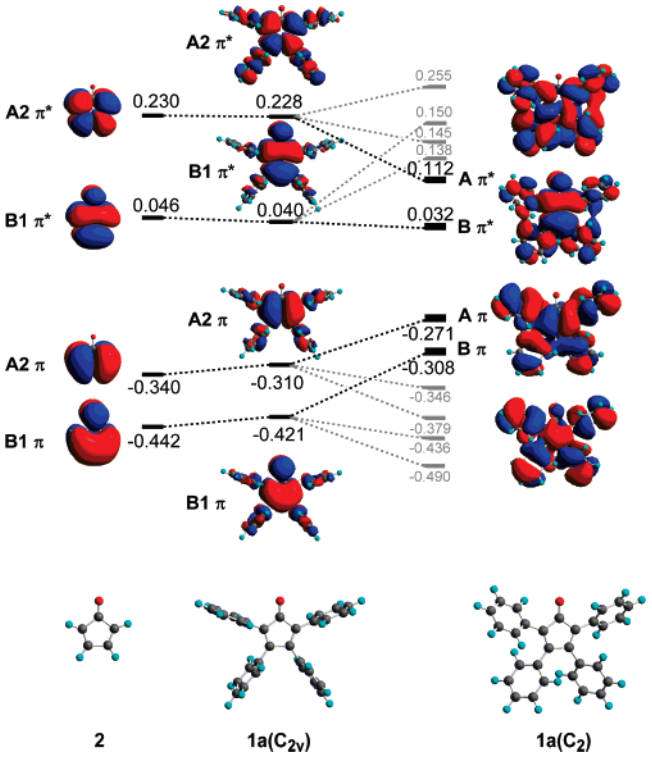

FIGURE 2. Correlation diagram of HF/6-31G(d) molecular orbitals of **2**, **1a(*C*$_{2v}$)** and **1a(*C*$_2$)**. Left: Upon substitution of the cyclopentadienone with orthogonal phenyl rings, the core π MOs remain nearly isoenergetic. Rotation of the phenyl rings to allow interaction of the π systems destabilizes the Aπ and Bπ while stabilizing the Aπ*. Note that the energy of the Bπ* orbital does not change significantly upon interaction with the pendent phenyl groups.

predominantly derived from the cyclopentadienone π MOs. As with many biaryl systems, the overlap between the adjacent π systems would reach its maximum when the two rings are coplanar, but this places the neighboring phenyl rings into van der Waals contact. The mixing of the π orbitals of the pendent phenyl rings destabilizes the A2π HOMO (which is now Aπ in the C_2 point group), and at the same time it stabilizes two other lower lying Aπ MOs (indicated by the gray lines in Figure 2). This mixing also stabilizes, albeit to a much lesser extent, the B1π* LUMO (now Bπ in the C_2 point group) while destabilizing two other higher lying Bπ MOs. Two other relevant cyclopentadienone π MOs are also affected by the interaction with the phenyl π MOs; the occupied B1π is greatly destabilized and the unoccupied A2π* orbital is greatly stabilized. The result is that these orbitals which were involved in the high intensity but short wavelength transitions in **2** become close enough in energy that at least three transitions involving these MOs move into the UV−vis region.

Plots of the total energy of **1a** as a function of θ as well as the energies of the highest occupied Aπ and lowest unoccupied Bπ* MOs are shown in Figure 3. To scan the relative total energy as a function of θ, all four phenyl ring dihedrals were constrained to be identical by the symmetry of the Z-matrix. Despite this artificial constraint on the geometry of **1a**, the minimum energy agrees well with the fully optimized B3LYP/6-31G(d) geometry and other maxima correspond to expected boundary conditions; **1a(*C*$_{2v}$)** exists as a local energy maximum, and the total energy of **1a** rises rapidly as θ approaches zero, which places neighboring phenyl rings in van der Waals contact. Changing the dihedral θ from orthogonality and increasing π interaction between the rings has a different effect on the energies of what are the HOMO and LUMO for **1a(*C*$_2$)**. Figure 4 shows that the HOMO is greatly destabilized as the π systems begin to interact, while the energy of the LUMO is essentially unchanged. This is presumably the result of the relatively small contribution of the phenyl π orbitals in the LUMO, as can be seen in Figure 2.

A thorough review of the UV−vis spectra of **2** and its theoretical description has been reported earlier along with other fulvene-like molecules.[30] Two major absorption bands were calculated at the INDO/S-CI level that matched observed absorptions,[15] a relatively weak absorption from the HOMO → LUMO (A2π → B1π*) transition of B2 symmetry, as well as a relatively strong HOMO → LUMO+2 (A2π → B1π*) transition also of B2 symmetry. These results were reproduced at the CIS/6-31G(d)//B3LYP/6-31G(d) level of theory, as shown in Table 2. The lower energy transition of B2 symmetry consisting of a HOMO → LUMO (A2π → B1π*) excitation is the same as that found in the INDO/S model. However, the stronger band was found at the higher level of theory to be a mixed transition of A1 symmetry consisting primarily of the HOMO-2 → LUMO (B1π → B1π*) excitation mixed with the HOMO → LUMO+1 (A2π → A2π*) excitation. Only seven transitions were reported in the INDO study, so up to 30 transitions were calculated in the present study. In this larger set of transitions, another was found consisting of a HOMO → LUMO+1 (A2π → A2π*) excitation, with a similar transition dipole moment, and at a slightly higher energy. Since the spectrum of **1a** has three absorptions, the identification of this third transition in the parent compound served as a reference point for the third transition present in **1a**.

1a(*C*$_{2v}$) is predicted to have the same transitions arising from the π MOs of the cyclopentadienone core as **2** (Figure 2), namely those consisting of the A2π → B1π*, B1π → B1π*, and A2π → A2π* excitations, along with many higher energy transitions associated with the phenyl rings. Again, the orthogonality of the π systems in **1a(*C*$_{2v}$)** prevents significant mixing of the central cyclopentadienone ring π orbitals with those on the pendant phenyl rings, which results in similar transitions to those found for **2**; the slight destabilization of occupied π MOs and the slight stabilization of the unoccupied π MOs lower the energies of the three transitions. The transition arising from the HOMO-1 → LUMO (B2σ → B1π*) excitation is A2 and is formally disallowed. The transition arising from the HOMO → LUMO+1 (A2π → B2σ*) excitation of B1 symmetry is allowed, but is predicted to have a near zero probability in the CIS/6-31G(d)//B3LYP/6-31G(d) model.

When **1a** is relaxed to C_2 symmetry, the preferred geometry at every level of theory examined, the same three major transitions are found at the CIS/6-31G(d)//B3LYP/6-31G(d) level of theory. Since the mixing of the phenyl π orbitals destabilizes the highest occupied B1π and A2π orbitals and stabilizes the lowest unoccupied A2π* orbital, the transition energies are all calculated to be smaller than those of **1a(*C*$_{2v}$)**. The transition arising from the HOMO → LUMO (Aπ → Bπ*) excitation remains present throughout the descent in symmetry from **2**, but becomes mixed with a transition from a lower lying orbital of like symmetry (see the Supporting Information for the full listing of the excitations involved) that also contains significant phenyl and cyclopentadienone π overlap. The HOMO → LUMO+1 (Aπ → Aπ*) and HOMO-1 → LUMO (Bπ →

(30) Buemi, G.; Zuccarello, F.; Raudino, A. *THEOCHEM* **1981**, *76*, 137.

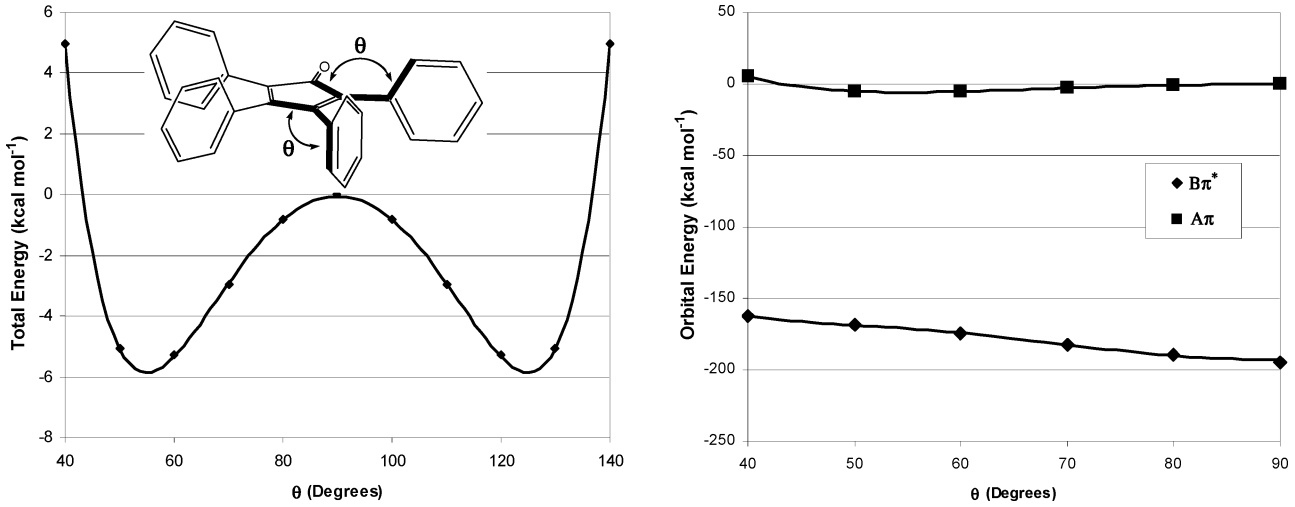

FIGURE 3. Phenylcyclopentadienone dihedral angular dependence of relative total energy and MOs of **1a**. Left: HF/63-1G(d) total energy of **1a** as a function of the four dihedral angles θ. The maximum at $\theta = 0°$ represents the lack of π overlap between the core and phenyl rings. Right: Highest occupied Aπ and lowest unoccupied Bπ* energies as a function of θ. As the dihedral decreases from orthogonality ($\theta = 90°$), the Aπ is destabilized while the Bπ* is nearly isoenergetic.

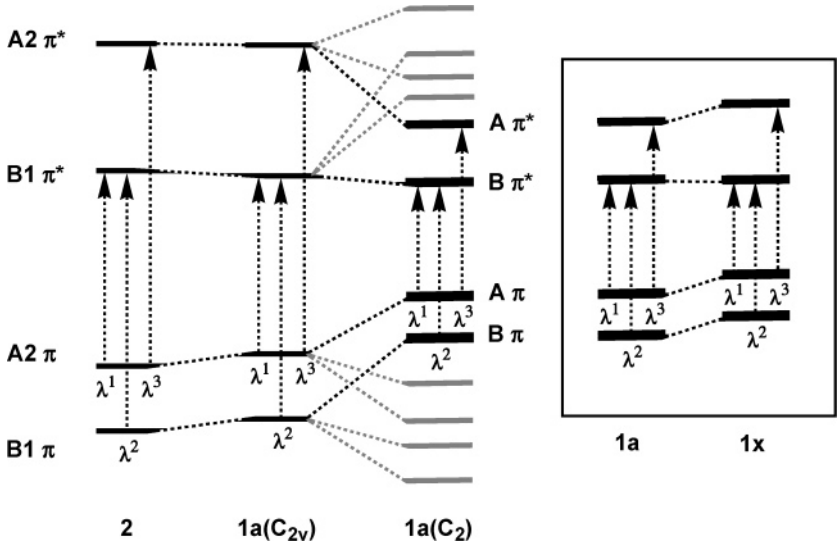

FIGURE 4. Assignment of λ^1, λ^2, and λ^3 to single electron excitations. Left: Effect of the phenyl substitution on the energies of the relevant orbitals and thus transitions: energies of all transitions are lowered. Right: Effect on the orbital energies of electron-donating substituents on the phenyl rings: energies of λ^1 and λ^2 are lowered, but λ^3 is not necessarily lowered.

TABLE 2. Electronic Transitions Calculated with CIS/6-31G(d) Corresponding to Absorption Maxima

	λ^1: A2$\pi \rightarrow$ B1π* [a]			λ^2: B1$\pi \rightarrow$ B1π*			λ^3: A2$\pi \rightarrow$ A2π*		
	E (kcal mol^{-1})	μ[b] (D)	c[c]	E (kcal mol^{-1})	μ (D)	c	E (kcal mol^{-1})	μ (D)	c
2	92.8	0.029	0.70	177.7	0.573	0.68	220.5	0.594	0.67
1a(C_{2v})	74.9	0.057	0.69	162.9	1.099	0.60	182.4	1.372	0.28
1a(C_2)	73.9	0.069	0.65	116.9	0.697	0.62	161.3	0.888	0.35

[a] Three major absorption maxima and their corresponding primary single electron excitation. [b] Electric transition dipole moment in Debyes. [c] Coefficient of indicated single electron excitation in overall wave function.

Bπ*) excitations mix, and give rise to a lower energy transition that is primarily the lower energy A$\pi \rightarrow$ Aπ* excitation and a higher energy transition that is primarily the B$\pi \rightarrow$ Bπ* excitation, although the latter has significant mixing of several other MO excitations.

Correlation of MO Energies and UV/Vis Spectra. To correlate the computed transitions with those observed in the spectra, computations were required on each of the eight TACPDs studied. However, the level of theory required to make a quantitative prediction of the electronic spectrum had to be determined. The transitions were identified at the CIS/6-31G(d)//B3LYP/6-31G(d) level of theory, and in principle more accurate energies could be obtained from a configuration interaction computation that includes doubles, triples, and quadruples or a multiconfigurational self-consistent field calculation such as a CASPT2[31] in which the active space includes

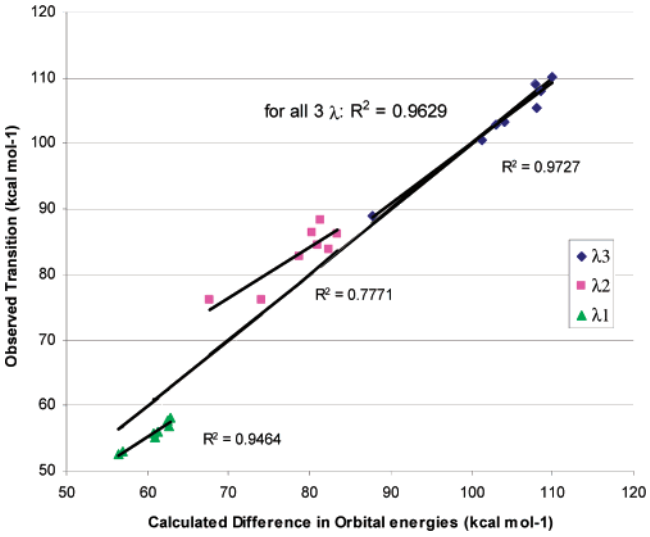

FIGURE 5. Correlation of the observed and calculated electronic transitions of **1a**−**h**, using B3LYP/6-31G(d) calculated MO energies.

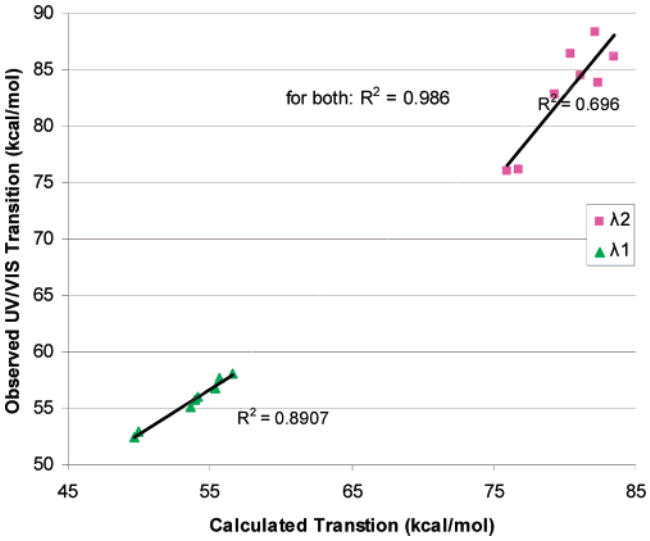

FIGURE 6. Correlation of the observed and calculated electronic transitions of **1a**−**h**, using TD-B3LYP/6-31G(d) calculated excitation energies.

the relevant π MOs. TDDFT could also be employed to calculate the lowest relevant electronic transitions. However, since each of the three transitions identified involves one predominant single electron excitation, it is reasonable to expect that there would be a correlation between the difference of the relevant orbital energies and the observed transitions.

The observed λ^1_{max} values show a linear correlation with the HOMO−LUMO gaps calculated for **1a**−**h**, as can be seen in Figure 5. The correlation was observed for the two levels of theory performed, the HF/6-31G(d) and the B3LYP/6-31G(d) methods. The correlation is best for the DFT method, with a linear least-squares fit having an R^2 value of 0.95, while for the HF methods, the R^2 value was 0.89. Higher levels of theory could be expected to give more accurate orbital energies or more detailed descriptions of the allowed optical transitions, but would not likely improve the fit of the experimental data to an extent that would justify the computational expense.

To demonstrate this, TDDFT (B3LYP/6-31G(d)) computations were carried out on **1a**−**1h** to determine the three electronic transition energies, and the linear least-squares correlation is 0.98, as is shown in Figure 6. While this is clearly a better correlation than that obtained for the simple DFT method, the TDDFT methods required 6−10 times more computational time, despite the calculation of only the three lowest energy transitions, which included only λ^1 and λ^2. A further comparison of the DFT MO method to the TDDFT shows that there is a larger systematic error in the DFT MO correlations; the largest computed error and average error for λ^1 for the DFT MO method are 5.9 and 4.9 kcal/mol, respectively, while they are 2.9 and 2.0 kcal/mol for the TDDFT method. However, if the systematic errors in both methods are compensated for by performing linear correlations of both data sets for λ^1, these errors are reduced to 1.2 and 0.5 kcal/mol for the DFT MO method and 1.1 and 0.4 kcal/mol for the TDDFT method. Recent TDDFT methodological studies have shown that the choice of functional and basis set—in particular 6-311+G-(2d,p)—can play a significant role in achieving high accuracy, to within 5 nm.[32] The MOs of **1a** were calculated at the B3LYP/6-311+G(2d,p) level, and the HOMO−LUMO gap was found to be 1 kcal/mol more accurate for λ^1, 0.5 kcal/mol less accurate for λ^2, and 3.5 kcal/mol less accurate for λ^3. While it is reasonable to expect that the more complete basis set may give more accurate MO energies for some if not all of the TACPDs discussed herein, the error inherent in approximating electronic transitions as single electron excitations may overwhelm this benefit. Similarly, alternative functionals may give more accurate energies, but this may not be reflected after the MO energy gap approximation is made.

At the B3LYP/6-31G* level, the two higher energy transitions, λ^2 and λ^3, also show a straight-line dependence on the calculated HOMO-1−LUMO and HOMO−LUMO+1 gaps, respectively. Not only do the values for each individual transition follow a well-behaved linear correlation with the computed MO gaps, but also all fall on the same line with a slope very close to one when plotted together, indicating that the DFT MO gaps are very good predictors of the actual UV/vis transitions across a large range of energies. A similar straight-line plot is obtained with the HF computed MO gaps, but with larger systematic errors. The straight-line correlations observed suggest that the three major electronic transitions for **1a**−**h**, and by extension **1a(C_{2v})** and **2**, are best described by the single electron excitations shown in Figure 4.

A major goal of this study was to identify a computationally inexpensive method to predict the electronic spectra of TACPDs. The correlations described above can now be compared to the VB models previously described by Becker and co-workers which proposed that the two longest wavelength transitions of **1a** correspond to the two charge transfer states depicted in Scheme 3, both of which eliminate the antiaromatic VB depiction of the ground state. The polarization of the CIS/6-31G(d) HOMO → LUMO excitation-derived transition is consistent with the polarization required for λ^1 in Scheme 3, and the same is true for the CIS/6-31G(d) HOMO-1 → LUMO

(31) Andersson, K.; Malmqvist, P.-Å.; Roos, B. O. *J. Chem. Phys.* **1992**, *96*, 1218. Serrano-Andrès, L.; Roos, B. O. *Chem.-Eur. J.* **1997**, *3*, 717.

(32) Jacquemin, D.; Preat, J.; Wathelet, V.; Perpète, E. A. *THEOCHEM* **2005**, *731*, 67. Jacquemin, D.; Preat, J.; Wathelet, V.; Fontaine, M.; Perpète, E. A. *J. Am. Chem. Soc.* **2006**, *128*, 2072. Jacquemin, D.; Preat, J.; Wathelet, V.; Perpète, E. A. *J. Chem. Phys.* **2006**, *124*, 074104.

SCHEME 3. Valence Bond Descriptions of Transitions λ^1 and λ^2

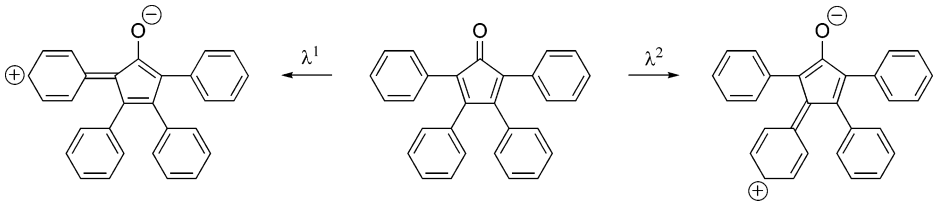

TABLE 3. Electronic Transitions Calculated with Modeling of Solvation CIS/6-31G(d) Corresponding to Absorption Maxima with Average (unsigned) Errors in kcal mol^{-1} and Largest Unsigned Error in Parentheses

	λ^1: A2π → B1π* [a]	λ^2: B1π → B1π*	λ^3: A2π → A2π*
B3LYP/6-31G*	4.8 (5.9)	4.7 (9.2)	1.0 (2.1)
SCRF B3LYP/6-31G*	4.9 (6.0)	4.3 (9.0)	1.0 (2.7)

[a] Three major absorption maxima and their corresponding primary single electron excitation.

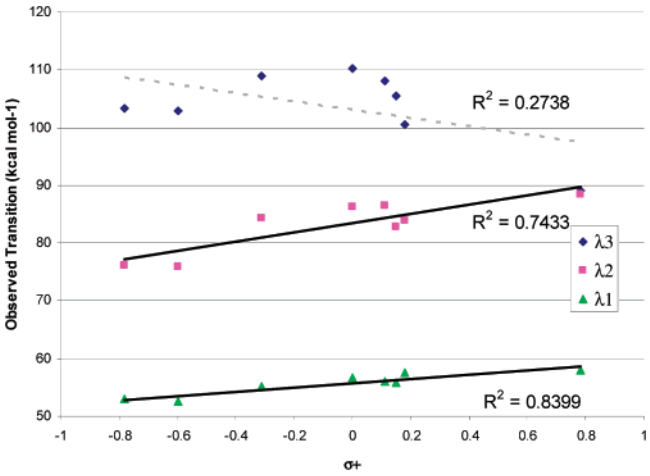

FIGURE 7. Correlation of observed electronic transitions with σ^+. Correlations are found for λ^1 and λ^2, but not for λ^3.

excitation-derived transition polarization and that required for λ^2. Thus, as has been stated earlier the valence bond versus molecular orbital theory dilemma is in fact an ill-posed one, and should be replaced by the notion that they are complimentary.[19]

Given the polarization suggested by the VB depictions and calculated at the CI and TDDFT levels, it is reasonable to consider the effect of solvation on the energies of the electronic transitions. SCRF B3LYP/6-31G* calculations were carried out on **1a**−**h**, and the results are shown in Table 3. Modeling of the solvation with the SCRF method did not improve the fit of the MO energy differences to the electronic transition energies appreciably. The straight-line correlation did improve slightly upon inclusion of the solvation effects, increasing R^2 from 0.978 to 0.984. Overall, this does not appear to be a significant enough improvement in the predictive power of the MO energy differences to justify the computational cost.

In the smaller set of TACPDs Becker and co-workers examined, the VB model was proposed because substitution of the 2- and 5-phenyl rings predominantly shifted the high wavelength absorption λ^1 and substitution of the 3- and 4-phenyl rings predominantly shifted λ^2. By examining a larger set of substituents, including some electron-withdrawing groups, perturbations of all three major transitions were observed. Although no 3- or 4-phenyl-substituted analogues were synthesized in the current study, computations of such analogues for which spectra had previously been recorded gave similar results to the **1a**−**h** series (see the Supporting Information).

While the DFT MO correlation to observed spectral absorptions is quantitative in nature, the simple and very elegant VB models described earlier are useful in making qualitative predictions, and the buildup of positive charge on the pendent phenyl rings in each VB description of the electronic transitions suggests that, as observed, electron-donating groups will stabilize the excited state while electron-withdrawing groups will destabilize the excited state, thereby blue-shifting the transition. This is exactly what is observed in the **1a**−**h** series, and it is reasonable to search for a simple parameter that captures the electron demand of the substituents as a model for the transition energies, and by extension, the HOMO−LUMO gap in these materials.

The plots of λ^1_{max} versus either Hammett σ values[21] or group electronegativities[20] gave random scatter, which suggested that the substituents were playing a greater role than just an inductive perturbation of the MOs involved in the transition. The σ^+ parameter[33] has been determined for different substituents in the ionization of phenyldimethylchloromethane where a formal positive charge is present at the *ipso* carbon. Such a positive charge resembles those in the charge transfer states shown in Scheme 3. A plot of σ^+ versus the λ^1_{max} values is shown in Figure 7, and although the correlation is not as precise as for the DFT MO method, it is still accurate enough to provide a rough prediction of the HOMO−LUMO gap for a TACPD substituted at the para positions of the 2- and 5-phenyl rings. The VB model also suggested that a charge transfer was involved in λ^2, and Figure 7 also shows a reasonable correlation between σ^+ values and the observed λ^2_{max} for **1a**−**h**. A similar plot for the λ^3_{max} values shows no such correlation, however. Examination of the MOs in Figure 2 shows that the Aπ LUMO has relatively little contribution from the pendent phenyl ring π orbitals, and as a result, the energy of this orbital changes to a lesser extent upon substitution of those phenyl rings. The other three relevant orbitals, the Bπ HOMO-1, the Aπ HOMO, and the Aπ* LUMO+1, have energies that change more upon substitution of the pendent phenyl rings. The result is that λ^1 and λ^2, which both involve excitation from a variable-energy MO to the relatively constant LUMO, show a stonger dependence on the phenyl substituents than does λ^3, which involves an excitation from and to MOs whose energies vary with substitution. This is shown in Figure 4, in which **1a** is substituted with electron-donating substituents to give a generic **1x**; λ^1 and λ^2 both decrease but λ^3 remains constant.

Conclusions

The dark purple color of the TACPDs arises from the very broad visible absorption band around 510 nm that has been

(33) McDaniel, D. H.; Brown, H. C. *J. Org. Chem.* **1958**, *23*, 42.

represented by a formal charge transfer absorption. CIS computations determined that this transition consists primarily of the HOMO to LUMO single electron excitation, and the good correlation of the DFT computed HOMO−LUMO gap with the observed absorptions of **1a**−**h** corroborated this assignment. Similar correlations of computed MO energy gaps to observed absorptions allowed assignment of two other electronic transitions to single-electron excitations. The use of this model is computationally less demanding than CI or CAS computations of the electronic transitions, and can serve as a relatively rapid screen for determining the shifts of TACPD HOMO−LUMO gaps arising from substitutions on the aryl rings, or in principle band gaps of larger molecules for which more detailed computations would be prohibitively costly. Perturbation and prediction of their HOMO−LUMO gaps are advantageous if these TACPDs are to be used as electronic materials. Though the production of high molecular weight oligomers is still under study, they may have utility as electronic materials due primarily to the tunable nature of the HOMO−LUMO gap of the monomer.

Experimental Section

1,3-Bis(4-nitrophenyl)-propan-2-one[34] **(3b).** 4-Nitrobenzyl bromide (0.956 g, 4.425 mmol), tetrabutylammonium iodide (0.186 g, 0.504 mmol), and tosylmethylisocyanide (0.432 g, 2.213 mmol) were dissolved in 50 mL of methylene chloride and the solution was stirred vigorously until the additives were completely dissolved. After 5 min, 20 mL of 40% aqueous NaOH was added and the reaction mixture was stirred as rapidly as possible for 4 h prior to neutralization with HCl. The resulting mixture was transferred to a separatory funnel and extracted with three portions of methylene chloride. Solvent was removed from the combined organic layers and dissolved in 8 mL of methylene chloride. HCl (1.0 mL, 50%) was added and the resulting red solution was stirred for 30 min. The hydrolysis was quenched with aqueous sodium bicarbonate and partitioned between water and methylene chloride. The organic layer was removed and the aqueous layer was extracted with three portions of methylene chloride. Chromatography (methylene chloride on silica gel) followed by recrystallization from ethanol/ethyl acetate gave the desired product (0.379 g, 57%, mp 178−179 °C). ^{1}H NMR δ 8.21 (d, J = 8.8 Hz, 4H), 7.34 (d, J = 8.8 Hz, 4H), 3.93 (s, 4H); ^{13}C NMR δ 201.9, 147.4, 140.4, 130.5, 123.9, 49.0; FTIR (neat, cm^{-1}) 1719.94, 1598.68, 1507.55, 1407.68, 1342.06, 1214.37, 1177.94, 1108.83, 1051.83, 1017.22, 855.29, 826.77, 790.06, 736.43, 707.67, 656.61, 631.25; PCIMS (m + 1)/z calcd 300.0746, found 300.2.

1,3-Bis(4-methoxycarbonylphenyl)propan-2-one[35] **(3c)**. Methyl-4-(bromomethyl)benzoate (1.169 g, 5.103 mmol), tosylmethylisocyanide (0.483 g, 2.47 mmol), and tetrabutylammonium iodide (0.231 g, 0.625 mmol) were dissolved in 35 mL of methylene chloride and the solution was stirred as rapidly as possible until it was completely homogeneous. After 5 min, 20 mL of 40% aqueous NaOH was added slowly to maintain the high stirring rate. The reaction was stirred vigorously for 4 h prior to neutralization with HCl. The resulting mixture was transferred to a separatory funnel and extracted with three portions of methylene chloride. Solvent was removed from the combined organic layers and dissolved in 8 mL of methylene chloride. HCl (1.0 mL, 50%) was added and the resulting red solution was stirred for 30 min. The hydrolysis was quenched with aqueous sodium bicarbonate and partitioned between water and methylene chloride. The organic layer was removed and the aqueous layer was extracted with three portions of methylene chloride. Two column chromatographic purifications (10% ethyl acetate in hexanes on silica) and subsequent recrystallization in ethanol and ethyl acetate provided the desired ketone (0.518 g, 62%, mp 139 °C). ^{1}H NMR δ 7.99 (d, J = 8.6 Hz, 4H), 7.21 (d, J = 8.6 Hz, 4H), 3.91 (s, 6H), 3.80 (s, 4H); ^{13}C NMR δ 203.7, 166.8, 138.7, 130.0, 129.6, 52.1, 49.2; FTIR (neat, cm^{-1}) 2954.86, 1707.01, 1629.29, 1575.20, 1510.58, 1434.35, 1416.32, 1275.18, 1177.10, 1100.14, 1052.23, 1017.73, 964.64; PCIMS (m + 1)/z calcd 327.1154, found 327.1.

1,3-Bis(4-(*tert*-butoxycarbonylamino)phenyl)propan-2-one (3d). 1,3-Bis(4-nitrophenyl)-propan-2-one (0.020 g, 0.067 mmol), Pd/C (0.014 g, 10 wt %), and di-*tert*-butyl dicarbonate (0.100 g, 0.458 mmol) were dissolved in 15 mL of ethyl acetate, to which 0.243 g (3.28 mmol) of $Ca(OH)_2$ was added. The reaction was agitated in a Parr shaker for 18 h under 58 psi of H_2. Column chromatography (hexanes on silica gel) gave the desired product (0.027 g, 99.9%, mp 127 °C). ^{1}H NMR δ 7.30 (d, J = 8.4 Hz, 4H), 7.05 (d, J = 8.4 Hz, 4H), 3.48 (br s, 2H), 3.63 (s, 4H), 1.51 (s, 18H); ^{13}C NMR δ 206.0, 152.7, 137.3, 130.0, 128.5, 118.8, 48.3, 28.3; FTIR (cm^{-1}, neat) 3329.69, 2926.12, 1717.64, 1699.84, 1593.93, 1520.14, 1456.90, 1413.86, 1391.91, 1366.25, 1317.50, 1231.95, 1152.17, 1051.44, 1051.44, 1018.35, 830.09, 771.11, 659.79, 503.45, 403.46; HRMS (m + Li)/z calcd 447.2489, found 447.2466.

2,5-Bis(4-nitrophenyl)-3,4-diphenylcyclopenta-2,4-dienone (1b). 3b (0.156 g, 0.520 mmol), benzil (0.471 g, 2.240 mmol), and potassium hydroxide (0.039 g) were dissolved in 10 mL of ethanol and the solution was brought to reflux for 2 h prior to cooling to room temperature and quenching with saturated ammonium chloride in 0.5% HCl. The aqueous layer was extracted with three portions of hexanes. Flash chromatography (5% ethyl acetate in hexanes) yielded **1b** as a bright purple crystalline solid (0.199 g, 81%, mp 245 °C). ^{1}H NMR δ 8.10 (d, J = 9 Hz, 4H), 7.41 (d, J = 9 Hz, 4H), 7.34 (t, J = 7.5 Hz, 2H), 7.24 (t, J = 7.5 Hz, 4H), 6.91 (dd, J = 8 Hz, 1 Hz, 4H); ^{13}C NMR δ 197.9, 157.5, 146.9, 137.0, 131.7, 130.8, 129.7, 129.0, 128.6, 124.2, 123.3; FTIR (neat, cm^{-1}) 3065.05, 2924.86, 2849.55, 1708.99, 1591.87, 1511.00, 1441.65, 1338.56, 1307.07, 1114.41, 862.99, 745.92, 718.01, 697.11; HRMS (m + Li)/z calcd: 481.1376, found 481.1357.

2,5-Bis(4-methoxycarbonylphenyl)-3,4-diphenylcyclopenta-2,4-dienone (1c). 3c (0.119 g, 0.365 mmol), benzil (0.102 g, 0.485 mmol), and potassium hydroxide (0.025 g) were dissolved in 10 mL of THF and the solution was brought to reflux for 2 h prior to cooling to room temperature and quenching with saturated ammonium chloride in 0.5% HCl. The aqueous layer was extracted with three portions of hexanes. Flash chromatography (5% ethyl acetate in hexanes on silica) yielded **1c** as a bright purple crystalline solid (0.084 g, 71%, mp 203−205 °C). ^{1}H NMR δ 7.91 (d, J = 8.2 Hz, 4H), 7.31 (d, J = 8.3 Hz 4H), 7.26−7.30 (m, 2H), 7.19 (t, J = 7.5 Hz 4H), 6.91 (dd, J = 8.5 Hz, 1 Hz, 4H), 3.89 (s, 6H); ^{13}C NMR δ 198.9, 166.8, 156.1, 135.2, 132.4, 130.0, 129.2, 129.1, 129.0, 128.9, 128.2, 124.9, 52.0; FTIR (neat, cm^{-1}) 2949.94, 1730.17, 1706.79, 1604.17, 1435.12, 1406.20, 1274.84, 1186.27, 1101.38, 1074.02, 1018.52, 959.01, 863.85; HRMS (m + Li)/z calcd 507.1784, found 507.1777.

2,5-Bis(4-(*tert*-butoxycarbonylamino)phenyl)-3,4-diphenylcyclopenta-2,4-dienone (1d). 3d (0.104 g, 0.264 mmol), benzil (0.115 g, 0.547 mmol), and potassium hydroxide (0.011 g) were dissolved in 10 mL of ethanol and the solution was brought to reflux for 2 h prior to cooling to room temperature and quenching with saturated ammonium chloride in 0.5% HCl. The aqueous layer was extracted with three portions of hexanes. Flash chromatography (5% ethyl acetate in hexanes) yielded **1d** as a bright purple crystalline solid (0.049 g, 30%, mp 137 °C). ^{1}H NMR δ 7.20−7.25 (m, 6H), 7.14−7.19 (m, 8H), 6.91 (dd, J = 8.3 Hz, 1 Hz, 4H), 6.44 (br s, 2H), 1.50 (s, 18H); ^{13}C NMR δ 200.9, 153.7, 152.5, 137.6, 133.3, 130.8, 129.2, 128.3, 128.0, 125.5, 124.4, 117.9, 74.7, 28.3; FTIR (neat, cm^{-1}) 3362.22, 2975.29, 2930.17, 1706.62, 1585.65, 1518.83, 1455.04, 1408.19, 1392.32, 1366.39, 1316.44, 1230.19, 1152.31, 1084.12, 1051.61, 1027.15, 846.49, 769.07, 730.46, 702.37; HRMS (m + Li)/z calcd 621.2941, found 621.2913.

(34) Campaigne, E.; Edwards, B. E. *J. Org. Chem.* **1962**, *27*, 3760.
(35) Inaba, S.; Rieke, R. D. *J. Org. Chem.* **1985**, *50*, 1373.

Computational Details. Geometry optimization of the cyclopentadienones was carried out with the Gaussian 03 software package[36] at the B3LYP/6-31G(d) level of theory,[37] and the minima were confirmed by the presence of no imaginary frequencies in frequency calculations. Single point energies were then calculated at the HF/6-31G(d)[38] level, using the B3LYP/6-31G(d) optimized geometry. Despite the failure of DFT methods for calculating eigenvalues and enthalpies of formation reported earlier for other large organic molecules[39] the B3LYP hybrid functional worked well with the rather simple geometries of the TACPDs. Prediction of the first 30 electronic states was performed by using a time-independent CIS[40]/6-31G(d) model, using a frozen core and direct calculation of integrals. The symmetry enforced structure of **1a-(C_{2v})** was optimized by a symmetry-constrained Z-matrix. The optimized parameters from this structure were then held fixed while all four of the pendent phenyl rings were rotated from $\theta = 90°$ to 0° to generate the energy plot in Figure 3.

Acknowledgment. We thank the University of Vermont for financial support of this work and Dr. Kelvin Chu in the Physics Department at the University of Vermont for computational cycles. Mass spectrometry was provided by the Washington University Mass Spectrometry Resource with support from the NIH National Center for Research Resources (Grant No. P41RR0954).

Supporting Information Available: Complete ref 25; NMR spectra; UV−vis spectra of novel compounds; detailed description of computational details including optimized Cartesian coordinates and/or Z-matrices for all TACPDs and CIS output for **2**, **1a(C_{2v})**, and **1a(C_2)**; plots of computed MO energy differences versus observed absorption spectra for the HF method and **1a**−**h**, and for the HF method and tetraphenylcyclopentadienones substituted at *p*-3-phenyl and *p*-4-phenyl from the literature. This material is available free of charge via the Internet at http://pubs.acs.org.

JO701676X

(36) Frisch, M. J.; et. al. *Gaussian 03*; Gaussian Inc.: Wallingford, CT, 2004.

(37) (a) Becke, A. D. *J. Chem. Phys.* **1993**, *98*, 5648. (b) Becke, A. D. *Phys. Rev. A* **1988**, *38*, 3098. (c) Lee, C.; Yang, W; Parr, R. G. *Phys. Rev. B* **1988**, *37*, 785.

(38) Roothan, C. C. J. *Rev. Mod. Phys.* **1951**, *23*, 69.

(39) Curtiss, L. A.; Raghavachari, K.; Redfern, P. C.; Pople, J. A. *J. Chem Phys.* **2000**, *112*, 7374.

(40) Foresman, J. B.; Head-Gordon, M.; Pople, J. A.; Frisch, J. *J. Phys. Chem.* **1992**, *96*, 35.